

# Automatic Spatially Dependent Parameter Selection for TV Denoising of MR Images with Non-Uniform Noise Distribution

Florian Knoll<sup>1</sup>, Yiqiu Dong<sup>2</sup>, Michael Hintermüller<sup>2,3</sup>, Rudolf Stollberger<sup>1</sup>

<sup>1</sup>Graz University of Technology, Institute of Medical Engineering, Graz, Austria

<sup>2</sup>University of Graz, Institute of Mathematics and Scientific Computing, Graz, Austria,

<sup>3</sup>Humboldt-University of Berlin, Department of Mathematics, Berlin, Germany

florian.knoll@tugraz.at

## Abstract

The Total Variation is a popular image model for denoising of MR images. The key problem in the application of the method is often the determination of a proper regularization parameter. This work presents an automatic strategy to determine a spatially dependent regularization parameter. It is shown that the method can be applied in cases where the distribution of the noise is uniform over the whole image, as well as in situations when this assumption cannot be made. The proposed algorithm is completely free of any user defined parameters and automatically adapts to different levels of corruption with noise and the existence of fine image features, which have to be preserved.

## 1 Introduction

The Total Variation (TV) is a popular regularization model in image processing [1]. It was also recently introduced for various applications in MR research. Examples include denoising and constrained image reconstruction [2]. In all TV based methods, a constrained optimization problem has to be solved that consists of two terms. A penalty term which enforces a low TV norm of the solution and a data fidelity term which ensures that the solution is consistent with the original data. A regularization parameter controls the tradeoff between the noise elimination and preservation of image details. Determination of the regularization parameter is often performed based on visual inspection of the reconstruction. This is a cumbersome and time consuming task and the results are always biased towards the personal preference of the user. Additionally, MR images are comprised of multiple details. In homogenous regions, a higher regularization can be performed than in regions which include multiple fine details. This indicates that it is desirable to apply different amounts of regularization based on the level of detail in a specific region. In this work spatially dependent regularization parameter selection for TV based denoising of MR images is introduced. With this technique, the regularization parameter is adapted automatically based on the details in the images. This improves the reconstruction of details while still providing adequate smoothing for the homogeneous parts. It is also demonstrated that this method can be used successfully in situations where the distribution of the noise is not uniform throughout the image, as it often occurs in combination with parallel imaging reconstruction of undersampled data sets [3, 4].

## 2 Theory

In order to enhance regions containing details while still sufficiently smoothing homogeneous parts, we improve the TV-model by using a spatially dependent regularization parameter instead of a scalar value only, i.e. we consider,

$$\min_u \frac{1}{2} \int_{\Omega} \lambda(x) |u - z|^2 dx + TV(u) \quad (1)$$

where  $z$  is the noisy image,  $u$  is the restored image, and  $TV(u)$  is the conventional TV penalty term [1]. In this model,  $\lambda$  is localized at image features. For small features, large  $\lambda$  leads to little smoothing so that details are usually preserved well. On the other hand, for large features, small  $\lambda$  leads to smoothing so that noise is removed considerably. Referring to [5], it can be shown that the minimization problem (1) is related to a constrained optimization problem of the type:

$$\begin{aligned} & \min_u TV(u) & (2) \\ \text{s.t.} & \int_{\Omega^\omega} |u - z|^2 dx \leq \sigma^2 |\Omega^\omega| \end{aligned}$$

for all windows  $\Omega^\omega$  with window size  $\omega$  in  $\Omega$ . Here,  $\sigma^2$  is the noise variance, estimated from the image. Compared with the common TV-model, the constraint in (2) is confined to each local region  $\Omega^\omega$  instead of the whole image. Considering a restored image  $u$  from the TV-model with a relatively small  $\lambda$ , the residual  $r = z - u$  will include noise as well as details. Then, the violation of the local constraint in (2) reflects the distribution of details in the image. Based on this, we define a statistic, “local variance

estimator”, as

$$\text{LVE}_{i,j}^{\omega} = \frac{1}{\omega^2} \sum_{(s,t) \in \Omega_{i,j}^{\omega}} (z_{s,t} - u_{s,t})^2, \quad (3)$$

where  $\omega$  is the window size. In general, whenever  $\text{LVE}^{\omega}$  is less than  $\sigma^2$ , i.e., the constraint in (2) is satisfied, it is assumed that in  $\Omega^{\omega}$  the residual primarily consists of noise. Otherwise, significant image details are left in the residual, and  $\lambda$  needs to be increased in order to preserve the details in the reconstruction. This adjustment depends on a robust upper bound for the (local) constraint. For this purpose, the confidence interval technique from statistics [6] is introduced to automatically adjust  $\lambda$  based on the size of the windows  $\Omega^{\omega}$ . This yields a parameter-free method, i.e., without necessity of manually tuning parameters. Moreover, the minimization problem in (2) is solved by a superlinearly convergent algorithm based on Fenchel-duality and inexact semismooth Newton techniques [5, 7].

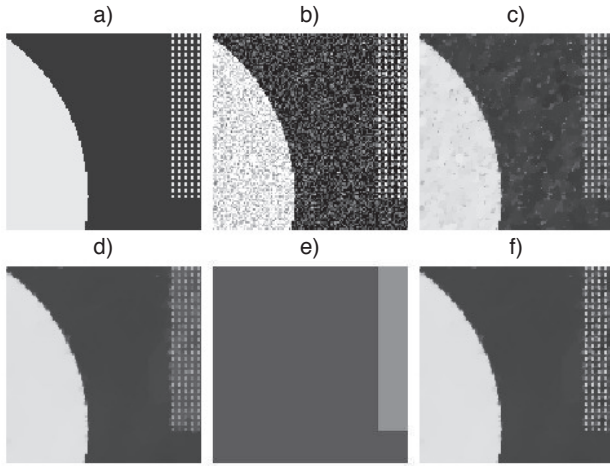


**Figure 1:** A numerical example of spatially variant regularization. (a) A numerical test image. (b) Noisy test image. (c) TV denoising with  $\lambda = 20$ . (d) TV denoising with  $\lambda = 10$ . (e)  $\lambda$  map:  $\lambda = 10$  (dark region) and  $\lambda = 20$  (bright region). (f) TV denoising with spatially variant  $\lambda$  from subplot (e).

The concept of spatially variant regularization is illustrated in Fig. 1 which shows the effect of different regularization parameters for a numerical test image. If the amount of regularization is too small, residual noise remains in the image. With higher regularization, noise is eliminated, but small image features start to disappear. The use of two different regularization parameters for the same image yields a result where noise is eliminated, and small features are preserved.

One limitation of this parameter estimation strategy is that it assumes that noise is uniformly distributed over the whole image. In reconstructions from undersampled data with parallel imaging [3, 4] which are nowadays widely used in daily clinical practice due to the pronounced reduction of scanning time, this assumption is violated. Reconstructed images show significant local noise amplifications

which depend on the configuration of the used coil arrays and their ability to separate pixels which are superimposed due to aliasing. This decrease of SNR due to noise amplification can be quantified by  $\text{SNR}_{\rho}^{\text{red}} = \frac{\text{SNR}_{\rho}^{\text{full}}}{g_{\rho} \sqrt{R}}$  [3]. The

factor  $\sqrt{R}$  only depends on the acceleration rate  $R$  and is the same for each pixel in an image. In contrast,  $g_{\rho}$ , the so called geometry (g)-factor, strongly depends on the coil geometry and takes different values for each pixel  $\rho$  in the image. If the method from equation (2) is now directly applied to these data sets, the algorithm will interpret these local noise amplifications as additional details in the image. This means that the regularization will be decreased in regions where the corruption with noise is higher. In order to prevent this, information about the spatial distribution of the noise amplification need be included in the parameter estimation process.

Since  $g_{\rho}$  shows the noise amplifications in reconstructed parallel images, the noise variance can be estimated as a multiple of  $g_{\rho}$ , i.e.,  $\sigma^2 = \iota g_{\rho}$ , where  $\iota$  is the noise variance in the background. Then, we restore the image iteratively by adjusting  $\lambda$  according to the following rule:

$$\begin{aligned} \tilde{\lambda}_{i,j}^{k+1} &= 2 \left( \tilde{\lambda}_{i,j}^k + \rho \max \left( \sqrt{(\text{LVE}_k^{\omega})_{i,j}} - \sigma_{i,j}, 0 \right) \right), \\ \lambda_{i,j}^{k+1} &= \frac{1}{\omega^2} \sum_{(s,t) \in \Omega_{i,j}^{\omega}} \tilde{\lambda}_{s,t}^{k+1}, \end{aligned} \quad (4)$$

where  $\rho = \|\tilde{\lambda}_k\|_{\infty} / \|\sigma\|_{\infty} > 0$  in order to keep the new  $\tilde{\lambda}_{k+1}$  at the same scale as  $\tilde{\lambda}_k$ . Initially, we assign a small positive value to  $\tilde{\lambda}$  in order to keep most of the details in the residual. After that, we restore the image iteratively, and keep increasing  $\lambda$  in the regions where the constraint in (2) is violated until the constraint is satisfied in all  $\Omega^{\omega}$ .

## 3 Methods and Results

### 3.1 Restoration of MR images with uniform noise distribution

In a first experiment, denoising was performed on a data set where the assumption of uniform noise distribution is valid, and the parameter estimation strategy from equation (2) can be applied directly. MR measurements of the brain of a healthy volunteer were performed on a clinical 3T scanner (Siemens Magnetom TIM Trio, Erlangen, Germany) using a 4 channel head coil. Written informed consent was obtained prior to the examination. A fully sampled  $T_2$  weighted turbo spin echo scan was used. Sequence parameters were repetition time  $\text{TR}=5000\text{ms}$ , echo time  $\text{TE}=99\text{ms}$ , turbo factor 10, matrix size  $(x,y)=(256,256)$ , 10 slices with a slice thickness of 4mm and an in plane resolution of  $0.86\text{mm} \times 0.86\text{mm}$ . The raw data set was exported from the scanner and complex Gaussian noise was added to the original  $k$ -space data of each individual coil. The standard deviation of the added noise was chosen such that the

ratio to the norm of the data was 1/40, 1/30 and 1/20. Afterwards, individual coil images were reconstructed with an inverse FFT and a sum of squares combination of the coils was performed. TV denoising was then performed with the proposed spatially variant parameter selection method (2). Fig. 2 displays noisy images, TV denoising results and the corresponding  $\lambda$  parameters from the experiments with uniform noise distribution.

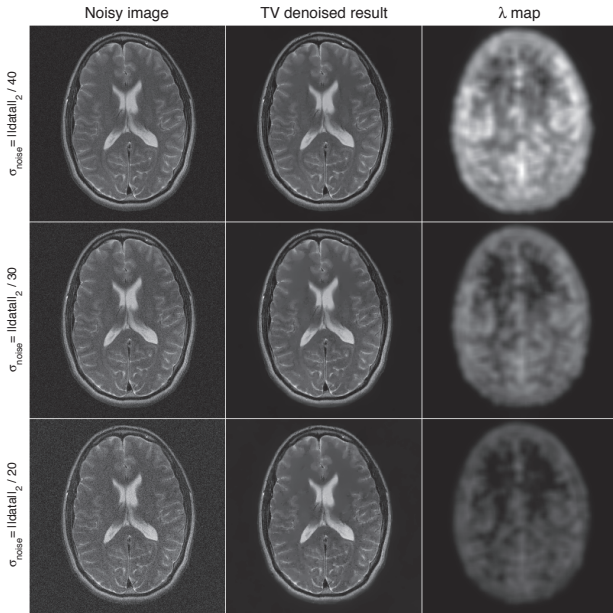


**Figure 2:** TV restoration results from MR brain data with uniform noise distribution. The images with noise (left column), the TV restorations and the regularization parameter maps are displayed for three different levels of SNR.

### 3.2 Restoration of parallel imaging reconstructions with non-uniform noise distribution

In the second experiment, parallel imaging reconstructions of the same dataset as in section 3.1 were investigated. Noise was again added to the original  $k$ -space data with a standard deviation of 1/50 with respect to the ratio to the norm of the data. Retrospective subsampling was performed by including only every second ( $R=2$ ) and every third ( $R=3$ ) line in row direction. 2D acceleration was simulated by performing factor 2 subsampling in both row and column direction, leading to total acceleration factor of  $R = 4$ . Coil sensitivity maps were obtained by dividing each individual coil image of the fully sampled data set by the sum of squares combination. Parallel imaging reconstruction was performed with a SENSE [3] based algorithm. This experiment was repeated 300 times. Noise amplification maps were obtained by calculating the standard deviation in each pixel over all 300 experiments. This was done for both unaccelerated and accelerated images.

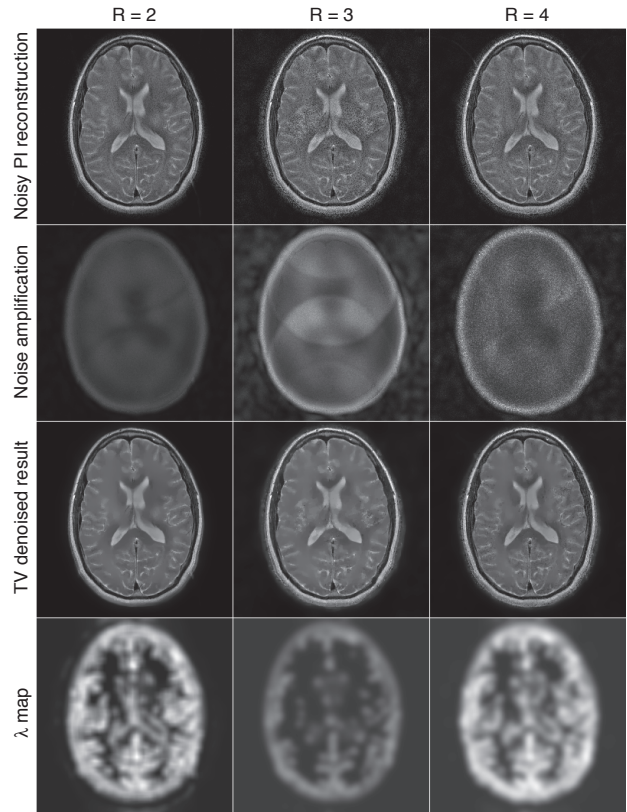


**Figure 3:** TV restoration results from undersampled parallel imaging MR data sets. Noisy images, parallel imaging noise amplification maps, TV restoration and the regularization parameter maps are displayed for three different levels of acceleration.

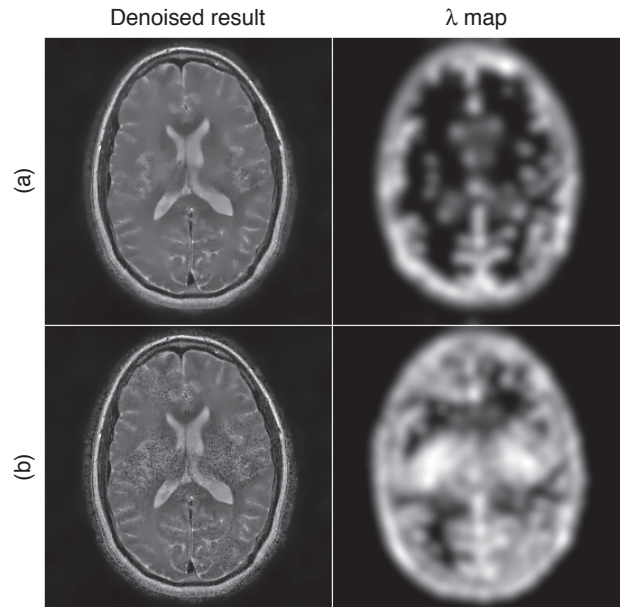


**Figure 4:** Comparison of denoising results for  $R=3$  accelerated parallel imaging reconstructions. Results with the proposed method (4) (a) and with the original formulation (2) (b) are shown.



The ratio of these two noise maps was used as an estimation of the noise amplification in the TV parameter estimation process. Noisy images, noise amplification maps, denoising results and the corresponding  $\lambda$  parameters are shown in Fig. 3.

Fig. 4 shows a comparison of the proposed method which includes information about the noise distribution with a direct application of (2), which assumes that the noise distribution is uniform for the case  $R = 3$  of Fig. 3.

## 4 Discussion

TV denoising efficiently eliminates noise in all investigated experiments while preserving fine image features. Bright values in the regularization parameter maps of Figs. 2, 3 and 4 correspond to high values of  $\lambda$ . This means that in these regions, the data fidelity term has a stronger influence on the solution and therefore the TV regularization is reduced. As expected, the algorithm decreases regularization in regions with a high amount of fine details. Additionally, the overall brightness of the parameter map is higher in images with less noise corruption (top row in Fig. 2, cases  $R = 2$  and  $R = 4$  in Fig. 3). This means that the overall amount of regularization is lower in these cases and illustrates, that the algorithm automatically adapts to the noise level in a particular image.

It is evident from the noisy images and the noise amplification maps in Fig. 3, that the assumption of a uniform noise distribution is violated in this case. Pronounced noise amplification occurs in specific regions of the images. The reason is, that the receive coils that were used during the parallel imaging reconstruction do not deliver sufficiently independent information in these regions. This is also the reason why noise amplification is higher for  $R = 3$  than for two dimensional  $R = 4$  acceleration because the sensitivities of the receive coils deliver equal amounts of independent information in the row and column direction. It can also be seen from the regularization parameter maps that the algorithm correctly identifies regions with a high amount of detail and reduces the regularization in these regions without being influenced by local noise amplification.

The parameter maps in Fig. 4 demonstrate that the original method (equation 2) decreases regularization in regions with high noise amplification (the parameter maps are brighter in these regions) because it is not able to separate them from locations in the image with a high amount of fine details. Therefore significant amounts of residual noise remain in the TV restoration. This problem does not occur with the proposed parameter selection strategy (equation 4).

While our experimental setup of repeating parallel imaging reconstruction 300 times is of course not suitable for practical application, this approach was chosen because it is the only established gold standard to estimate noise in parallel imaging. The SENSE theory [3] also allows to make theoretical predictions about noise amplifications based on

the used coil geometry. The use of such g-factor maps in the proposed method is the subject of current investigations. Future work will also include the extension of the proposed method to the problem of constrained image reconstruction [2].

One of the most important features of the proposed parameter selection strategy is that it is completely independent of any user defined parameters. While regularized image reconstruction and image denoising have been very active fields in MRI research during the last years, selection of the regularization parameter is still based on visual inspection of the results in many cases, and surprisingly little work has been done as regards this subject. Our results have shown that automatic estimation of spatially dependent regularization parameters leads to excellent results in MR image denoising and that the algorithm automatically adapts to data sets with different amounts of noise level and fine details.

## Acknowledgements

This work was supported through project SFB F3209 granted by the Austrian Science Fund.

## References

- [1] L. I. Rudin, S. Osher, and E. Fatemi, "Nonlinear total variation based noise removal algorithms," *Phys. D*, vol. 60, no. 1-4, pp. 259–268, 1992.
- [2] K. T. Block, M. Uecker, and J. Frahm, "Undersampled radial MRI with multiple coils. Iterative image reconstruction using a total variation constraint." *Magn Reson Med*, vol. 57, no. 6, pp. 1086–1098, Jun 2007.
- [3] K. P. Pruessmann, M. Weiger, M. B. Scheidegger, and P. Boesiger, "SENSE: sensitivity encoding for fast MRI." *Magn Reson Med*, vol. 42, no. 5, pp. 952–962, Nov 1999.
- [4] M. A. Griswold, P. M. Jakob, R. M. Heidemann, M. Nittka, V. Jellus, J. Wang, B. Kiefer, and A. Haase, "Generalized autocalibrating partially parallel acquisitions (GRAPPA)." *Magn Reson Med*, vol. 47, no. 6, pp. 1202–1210, Jun 2002.
- [5] Y. Dong, M. Hintermüller, and M. Rincon-Camacho, "Automated parameter selection in a multi-scale total variation model," iFB-Report No. 22 (11/2008), Institute of Mathematics and Scientific Computing, University of Graz.
- [6] A. Mood, *Introduction to the Theory of Statistics*. McGraw Hill, 1974.
- [7] M. Hintermüller and G. Stadler, "An infeasible primal-dual algorithm for total bounded variation-based inf-convolution-type image restoration," *SIAM Journal on Scientific Computing*, vol. 28, no. 1, pp. 1–23, 2006.